(π^+,p) and (π^+,d) reactions on light nuclei

K. G. R. Doss,* P. D. Barnes, N. Colella, S. A. Dytman,†
R. A. Eisenstein, C. Ellegaard,‡ F. Takeutchi,§ and W. R. Wharton
Carnegie-Mellon University, Pittsburgh, Pennsylvania 15213

J. F. Amann
Los Alamos Scientific Laboratory, Los Alamos, New Mexico 87545

R. H. Pehl and A. C. Thompson
Lawrence Berkeley Laboratory, Berkeley, California 94720
(Received 9 March 1981)

The (π^+,p) and (π^+,d) reactions on $1p$ shell nuclei are studied between $T_\pi=32$ and 81 MeV. Cross sections both to the continuum and to discrete two body final states are given. The spectra and angular distributions of the (π^+,p) continuum are examined in terms of a two-nucleon pion absorption mechanism. The $^{12,13}C(\pi^+,p)$ spectra of discrete states are similar to the corresponding $^{12,13}C(p,d)$ spectra at the same momentum transfer. The $^{16}O(\pi^+,p)^{15}O$(g.s.) transition is found to have an abnormally small cross section relative to other transitions of similar spectroscopic strength. The two-neutron pickup (π^+,d) data to discrete states is the first published data on this reaction. The (π^+,d) reaction is found to favor strongly transitions in the $1p$ shell of angular momentum transfer $L=2$. The relative strength of these $L=2$ transitions varies the same way as the corresponding (p,t) cross sections. No $L=0$ transitions are clearly identifiable. The (π^+,d) angular distributions are compared to the calculations of Betz and Kerman. The calculations reproduce well the absolute magnitude and shape of the (π^+,d) angular distributions but fail to predict the L dependence, pion energy dependence, and possibly even the spin transfer dependence of the (π^+,d) cross sections.

[NUCLEAR REACTIONS $^{12,13}C$, $^{16}O(\pi^+,p)$, ^7Li, ^{10}B, $^{12,13}C$, $^{16,18}O(\pi^+,d)$ $E=32-81$ MeV; measured spectral shape, $\sigma(\theta)$ for continuum and discrete states.]

I. INTRODUCTION

This report is a presentation of low energy pion absorption data on light nuclei involving the final states: (i) single proton emission, (ii) single deuteron emission, (iii) inclusive proton emission, and (iv) inclusive deuteron emission. Our understanding of the pion absorption process is still at a rudimentary stage, even though it is basic to pion-nucleus physics. Pion absorption is a significant part of the total pion-nucleus reaction cross section and has strong interplay with both elastic and inelastic scattering. The (π^+,p) or (p,π^+) reaction to discrete two-body states has provided the most abundant data on pion absorption but is still far from being understood theoretically.[1] One advantage of obtaining a large amount of (π^+,p) data is that the detailed systematic behavior of the reaction can be studied while changing many of the variables, for example, the pion energy and the target nucleus. A partial compilation[2] of the data, including the data in this report, reveals simple systematic behavior which is suggestive of a pion absorption on two nucleons rather than a simple neutron pickup process. Not as much data has been obtained for other pion annihilation reactions, primarily because most existing data have been obtained with magnetic spectrometers which are highly selective in what they measure. In contrast, the germanium crystal spectrometer used in our experiment allowed us to examine a large sample of pion annihilation products simultaneously. We measured (π^+,p) inclusive data to the continuum which is a large fraction of the pion absorption cross section and should be of value in determining gross features of the absorption process. Studies[3,4]

underway in this direction have not provided a simple interpretation of the gross features of the data. Either the basic absorption process is complicated or else the pion and the reaction products penetrate far into the nuclear volume and are greatly distorted by the nuclear medium.

We also examined the (π^+,d) reaction to discrete states which is a miniscule part of the total annihilation cross section. Nevertheless, the (π^+,d) reaction may give us new clues about the way a pion annihilates inside a nucleus. One of the goals of this paper is to compare several different pion annihilation reactions. Such comparisons may be valuable because even the most basic questions about pion absorption are not yet convincingly answered.

Another reason to study pion absorption is that it can be used to examine unexplored regions of nuclear structure. As a case in point, the (π^+,d) reaction removes from the nucleus two neutrons with small relative (internal) momentum but large (~ 800 MeV/c) center-of-mass momentum with respect to the rest of the nucleus. (Such large-momentum two-neutron removal processes have never been examined before.) It will be interesting to learn if the coherent enhancement due to pairing correlations observed in certain low energy (p,t) two-neutron pickup transitions also persists at large momentum transfer. Unfortunately, the (π^+,d) cross sections to discrete states are very small. This is partially due to the short mean free path of the deuteron combined with the large angular momentum mismatch of the pion and deuteron. The former inhibits a volume reaction whereas the latter inhibits a surface reaction. [However, as mentioned above, the small cross section could also be partially attributable to the (π^+,d) reaction sampling a small but interesting part of the nuclear structure.] It is our hope that these first (π^+,d) data will stimulate more theoretical work to address these questions. (This paper is limited to the presentation of the data and a brief exploration of its features in light of the existing theories.)

II. EXPERIMENTAL DATA

A. Experimental overview

This experiment was done at the Clinton P. Anderson Meson Physics Facility (LAMPF) using the low energy pion (LEP) beam line.[5] We used a stack of eight high-purity germanium crystals to detect the particles scattered from the target. Three multiwire delay line proportional chambers were used to calculate the trajectory of the particle from the target to the detector. Veto scintillators surrounded the germanium detectors to reject the particles that did not stop in the crystals. Two ionization chambers downstream of the target monitored the intensity of the incident pion beam. A three-scintillator telescope sitting at a backward angle looked at the particles scattered from the target and provided an additional beam monitor. The overall setup is similar to the one used in (π,π') experiments,[6] and is shown schematically in Fig. 1.

The ^{7}Li and ^{12,13}C and $(CH_2)_n$ targets were 0.15 to 0.5 gm/cm^2 thick. The 0.48 gm/cm^2 86% enriched ^{13}C target was made from ^{13}C powder with kraton binder by the WX-2 division of Los Alamos Scientific Laboratory (LASL). The ^{10}B target was a powder enclosed between Mylar sheets. D_2O and H_2O (either ^{16}O or 98% enriched ^{18}O) water targets were made by gluing stretched 1 mil Mylar to each side of a stainless steel frame, and filling with a syringe.

The uniformity of thickness of the liquid targets was determined by measuring the relative attenuation of beta rays from a strontium source through the different parts of the target. The initial nonuniformity in the thickness was about 10% for the 0.24 to 0.55 gm/cm^2 targets. It worsened by a factor of 2 or more after several days due to stretching of the Mylar, thereby requiring a frequent change of the target.

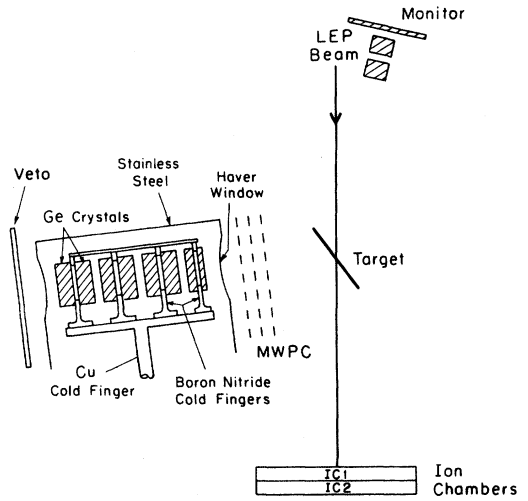

FIG. 1. A schematic (not to scale) diagram of the apparatus used in the experiment. The monitor telescope is in the vertical plane 60° from the horizontal.

B. Germanium detectors

The germanium detector stack used in this experiment was developed by the semiconductor detector group at Lawrence Berkeley Laboratory in consultation with Carnegie-Mellon University. The detector consists of a stack of eight cylindrical high-purity germanium crystals of diameter approximately 4 cm and thicknesses ranging from 0.25 to 1.2 cm. The crystals are mounted in pairs on boron nitride cold fingers which are placed on a copper plate. The plate is cooled to near 77 K by a copper rod which is in a liquid nitrogen dewar. The boron nitride cold fingers have a 3.5 cm diameter hole in the center to let particles pass through.

The total effective thickness of this stack is about 8 cm of germanium. With this we can detect pions of maximum energy of 100 MeV, protons of 200 MeV, and deuterons of 300 MeV. The minimum energy to identify these particles is determined by the thickness of the first crystal in the stack, which is 0.25 cm. This implies a minimum energy of 15 MeV for pions, 30 MeV for protons, and 50 MeV for deuterons.

Each detector is electrically isolated with a separate preamplifier. The signal from each preamplifier is shaped two ways by an amplifier giving a slow linear signal with risetime 0.8 μs and a fast linear signal with 0.2 μs risetime. The slow linear signal is used for the energy measurement and is sent to a stretcher-multiplexer which feeds all the signals in sequence to an 8192 channel analog to digital converter (ADC). The fast linear signal is fed into a peak-sensing ADC. Its purpose is to reject pile-up events by requiring that the slow and fast linear signals be consistent with each other. Rejecting pile-up events was especially important for the deuteron spectra because of the small cross section for producing deuterons and the large number of proton and pion events which can simulate deuterons if pileup occurs. For example, in the $^{12}C(\pi^+,d)^{10}C$ 65 MeV, 30° spectrum (Fig. 15) the pile-up rejection removed two events per every 10 MeV of the spectrum. For protons, pileup is not a significant problem.

In measuring the energy of charged particles using this detector, inaccuracies can arise in the following ways: (i) if the particle, through Coulomb multiple scattering, escapes from the stack without depositing all its energy; (ii) if it loses a significant portion of its energy in the Li contact dead layers on one face of each crystal; (iii) if it passes through a "cold finger" in going between crystals; (iv) if it has a nuclear interaction in a crystal; (v) if it decays and a varying amount of energy is deposited in the crystals by its decay products.

We estimated the contribution of multiple scattering to the efficiency using a Monte Carlo code ANGLE.[7] The program ANGLE simulates the passage of particles through a stack of detectors taking into account the Coulomb multiple scattering of particles and energy loss straggling. It includes the effects due to dead layers and cold fingers and ignores the effects due to nuclear interactions and particle decay. We obtain the efficiency correction for nuclear interactions from previous measurements of nuclear reaction cross sections for the various particles.[8] For pions, we assume that the nuclear reaction cross section is about the same as that for protons. We estimate the loss of pions due to π-μ-e decay to be 15% based on analysis of data taken with the detector in a low intensity pion beam. From these factors, we can calculate the total efficiency for detecting the particles as a function of its energy. The result of multiple scattering calculations show that the efficiency to detect particles of a given type decreases as its energy and range increases. Due to the effect of the cold fingers, the efficiency has a staircase shape as a function of incident energy, remaining approximately constant for particles stopping in the same crystal. The highest energy pions (80 MeV), protons (150 MeV), and deuterons (150 MeV) detected in this experiment have absolute detection efficiencies of about 40%, 50%, and 60%, respectively.

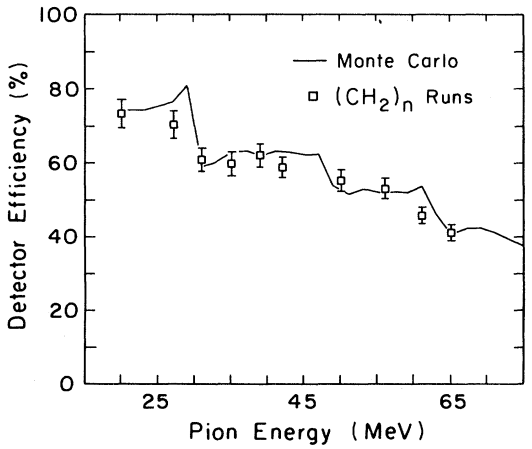

FIG. 2. The measured energy dependence of the pion detection efficiency using the germanium crystals. The normalization is adjusted to agree with the Monte Carlo calculation (solid line). The experimental points, but not the Monte Carlo, are averaged over several MeV.

There are a few methods by which we can experimentally check our efficiency calculation. The energy of elastically scattered pions from protons (in a polyethylene target) varies with scattering angle; using this and the known differential cross section for the scattering,[9] we can determine the relative variation of pion detection efficiency with pion energy. To cover the full pion energy range of interest it is necessary to choose several incident pion energies. Figure 2 shows that this measured efficiency is consistent with the staircase shape of the efficiency from the Monte Carlo calculation.

The Monte Carlo calculation shows more structure than the measured efficiency because the experimental points are averaged over several MeV. However, the step in the efficiency at some of the crystal interfaces has been qualitatively verified experimentally by putting a series of ^{12}C slabs of various thickness in front of crystal 1. The energy straggling in the slabs shifts the pion elastic peak across the interface allowing us to measure the energy dependence of the efficiency. A clearly visible stepshape in the efficiency is seen. However, this method is not quantitatively accurate because the multiple scattering in the ^{12}C slabs can also affect the efficiency.

Another method used to check our efficiency calculations was to detect the protons from the $\pi^+d\rightarrow pp$ reaction at a forward angle and at the complementary back angle. The cross sections for these two angles are kinematically related and the efficiency variation with proton energy can be checked without knowledge of the $\pi^+d\rightarrow pp$ cross section. This was done at complementary angles of 37 and 106 deg for an incident pion energy of 105 MeV. This determines the ratio of the proton efficiencies for 84 and 150 MeV to be $\epsilon(150)/\epsilon(84)=0.73$, which is consistent with the calculated ratio of 0.68 to within 10%.

A third method to check the multiple scattering part of the Monte Carlo code is to use the multiwire chamber information on trajectories and make radius cuts on the impact location of the events in the first crystal. Correcting for the change in solid angle, we can determine the efficiency dependence on the impact location. The results agree to 10% with the Monte Carlo calculation.

Using these efficiency calculations the absolute cross section is obtained either by measuring and normalizing to the π^+p elastic scattering cross section obtained from the Dodder phase shifts[10] or to the known $\pi^+d\rightarrow pp$ cross sections.[11] When both normalizations were used they were found always to agree to within the experimental error of about 15%.

The Ge crystals are oriented pair wise such that the Li contact dead layers (50–100 μm) on crystals 2 and 3, 4 and 5, and 6 and 7 face each other. The energy loss in a dead layer cannot be corrected for if the particle stops in the dead layer. However, for those particles which pass through the dead layer and deposit energy in the next crystal a correction can be made. This is shown in Fig. 3. Figure 3(a) shows the measured total energy spectrum of the Ge crystals when placed in a low intensity proton beam. The proton beam energy is adjusted so that most protons stop near the 2, 3 dead layer. Figure 3(b) shows the same data restricted to events depositing at least 0.5 MeV in crystal 3. We can see that the measured energy of these protons is up to 5 MeV less than events stopping in crystal 2, even though the beam is nearly monchromatic. By comparing the counts in Figs. 3(a) and 3(b) we see that only a fraction of the events with smaller measured energy stop in crystal 3. The others stop in the dead layer.

If E is the energy of the particle before it enters the dead layer, and E' the energy measured in crystal 3, then the particle identification parameter, P, is given by the equation

$$P=(E^{\alpha}-E'^{\alpha})/D\ , \tag{1}$$

where D is the total thickness of the dead layers at the 2, 3 interface and α was set equal to 1.73.

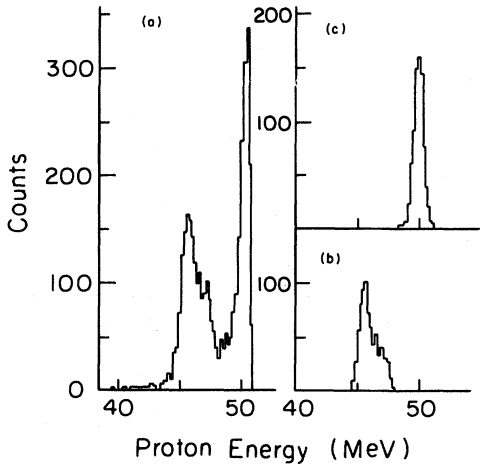

FIG. 3. Spectra obtained by placing the germanium detector in a 50 MeV proton beam. (a) All events; (b) events stopping in crystal 3; (c) the corrected energy [Eq. (2)] for events stopping in crystal 3.

Solving for E,

$$E=(E'^{\alpha}+PD)^{1/\alpha}. \quad (2)$$

The utility of the in-beam spectrum is now obvious. We can adjust the value of D so that the corrected energy for the proton going through the dead layer is the same as the energy of the proton that did not enter the dead layer, thus determining the dead layer thickness. Figure 3(c) shows the corrected spectrum with $D=0.020$ cm of Ge. This determination of D has uncertainties due to straggling in energy loss and an accuracy of $\pm 20\%$ is expected. Since the dead layer corrections to energy are usually less than 1 MeV, the error in corrected energy is quite small. Once D is determined, Eq. (2) gives the corrected energy for any particle.

The major problem with dead layers is that they distort the spectrum in several well-defined regions. Events which stop in the dead layer cannot be energy corrected and their energy will be shifted by the amount of energy deposited in the dead layer. This shift of events to lower energy leaves a narrow hole in the spectrum. This is most noticeable for the crystals 2, 3 interface as seen in Fig. 5 near 50 MeV. For higher interfaces, the straggling smears out the effect and it is much less noticeable.

The particle identification, for a particle reaching the nth crystal, can be calculated n-1 ways by choosing D in Eq. (1) as the thickness of either the first 1, 2,...n-1 crystals and defining E' as the energy deposited in the last n-1, n-2,...1 crystals, respectively. Requiring all P's to agree results in a clean particle identification spectrum. For example, the P spectrum for particles stopping in crystal 4 is shown in Fig. 4.

The energy calibration of the signals from each Ge crystal was obtained by a two stage process. First high gain was used on the amplifier and the peak positions of known γ sources, ^{137}Cs, ^{60}Co, and ^{22}Na, was measured to determine the energy calibration at this gain setting. An electronic pulser was then used to measure the change of the energy calibration when the amplifier gain was reduced to the experimental condition. The calibration had a typical error of 1%, but the peaks in the proton spectra are readily identifiable with the known levels of the residual nucleus and the lack of a more accurate calibration was not a major problem. For the deuteron spectra the low cross section and poor statistics require that we know the peak positions independently. An empirical procedure based on

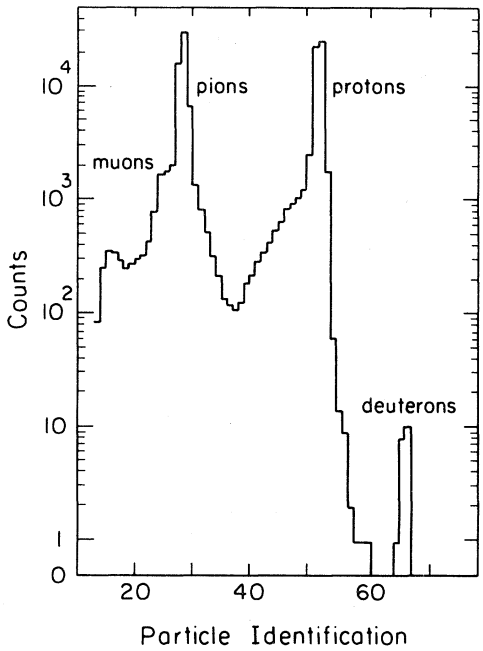

FIG. 4. A particle identification spectrum for particles stopping in crystal 4.

the known observed peaks in the proton and pion spectra was used to predict the locations of the expected peak positions in the deuteron spectra. This was also effectively corrected for straggling losses in the target, air, etc. The error in the predicted location of the (π^+,d) transitions is estimated to be about 0.5 MeV. In fact all our (π^+,d) spectra are well described by our calibration procedure using the (π^+,p) peak positions.

III. THE (π^+,p) AND (π^+,d) CONTINUUM DATA

The continuum data are a large fraction of the pion annihilation events and could reveal gross features of the absorption process. Recently McKeown *et al.*[4] using (π^+,p) continuum data between $T_\pi=100$ and 220 MeV have shown that the effective number of nucleons, N, sharing the momentum and energy of the annihilated pion is 3 for $A=12$ and increases to 5.5 for $A=181$. Doss and Wharton[12] have examined the A dependence (near the 3-3 resonance) of (1) the total pion absorption cross section, (2) the effective number of nucleons sharing the pion momentum and energy, and (3) the proton yields from π^+ and π^- induced reactions. They show that the A dependence can be explained by basic geometrical arguments assuming the pion penetrates the nuclear volume and

annihilates on a pair of nucleons. Additional nucleons become involved in the process through final state interactions of the two outgoing nucleons.

An alternative model for describing both the McKeown data and also the shape of some proton spectra is given by Ko and Bohrman.[13] Their model views the annihilation process as a pion interacting with a single nucleon, which becomes a Δ, and moves forward through the nucleus. This so-called "leading particle" multiple scatters off other nucleons. There is a free parameter, Q, which is the probability that no pion is emitted during each successive interaction of the leading particle ($Q \simeq 0.9$). Only the multiple scattering of the leading particle is treated and they assume secondary particles escape without final state interactions. This model also describes the data very well.

Ko and Bohrman assume a reaction mechanism very different from that of Doss and Wharton. However, both models reproduce the data by using the geometrical concept of multiple collisions of particles following straight line trajectories through the nucleus. It is probably safe to assume from the data that multistep collisions are taking place. Unfortunately the dominance of multistep collisions makes it harder to study the basic pion annihilation process. Therefore we have concentrated on light nuclei to try to minimize the multistep nature of the reaction. Specifically, the inclusive $^{12}C(\pi^+,p)$ spectral shape, angular distribution, and energy dependence are examined to investigate the compatibility of the data with the model of a pion annihilating on a quasideuteron to produce two high energy protons: $\pi^+ d \rightarrow pp$. However, even in a light nucleus, ^{12}C, the multistep processes appear to be dominating the data, preventing any definitive conclusions about the reaction mechanism.

Two proton energy spectra for incident 34 MeV pions are shown in Fig. 5. In general they show a smooth distribution. The dip seen at about 50 MeV in the proton spectra is an experiment artifact due to protons stopping and depositing energy in the dead layer between the 2nd and 3rd crystals (see Sec. II B). Fewer than half of the missing events in the dip are shifted to lower energy. The other events stopping in the dead layer are rejected by a strict particle identification requirement. These two spectra at 30° and 90° along with spectra at intermediate angles show a broad bump which moves to smaller energy with increasing angle. The bump peaks at about 88.5 MeV at 30° and at about 60 MeV or less at 90°. The energy of the bump moves with scattering angle at a faster rate

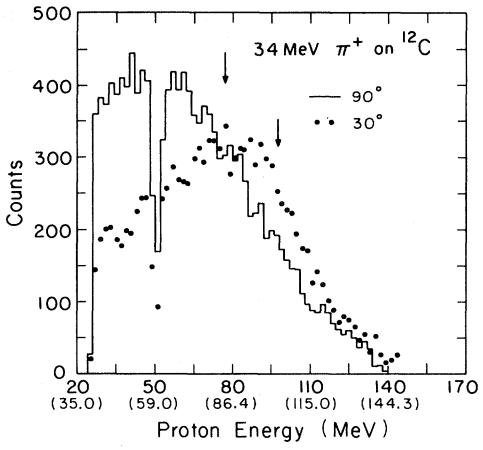

FIG. 5. Proton spectra for 34 MeV pions interacting with ^{12}C taken at $\theta = 30°$ (dots), 90° (histogram). The dip near 50 MeV is due to a dead layer (see Fig. 2). The energy scale is given as the measured energy and, in parenthesis, the energy corrected for the straggling of the proton through half the target and other material before the detector. This correction is nearly the same for both angles. The arrows locate the $^2H(\pi^+,p)$ energy at 90° and 30°.

than the $\pi^+ d \rightarrow pp$ reaction would indicate. A comparison with the $\pi^+ d \rightarrow pp$ kinematics shows the bump to be 15 ± 2 MeV too low at 30°, 18 ± 2 MeV too low at 50°, and at least 24 ± 5 MeV too low at 90°. Only part of this missing energy could be due to the binding energy of a quasideuteron in ^{12}C. For example, an unrealistic binding energy of 29 MeV would be needed to explain the missing 15 MeV at 30°. The low energy of the bump could be accounted for by allowing the pion to annihilate on a cluster of three or more nucleons. However, the kinematic shift of the bump is characteristic of a lighter system of less than two nucleon masses. To resolve these two features of the data, a multistep reaction mechanism is almost certainly needed.

Therefore, if $\pi^+ d \rightarrow pp$ is the dominant process the protons must scatter off other nucleons before leaving the nucleus. In a two nucleon absorption process the two nucleons are expected to recoil at nearly 180° with respect to each other. If the reaction takes place on the nuclear surface, one of the nucleons would always escape without passing through the nucleus. In this situation we would expect to see a dominant peak in the proton energy spectrum at the energy predicted by the $\pi^+ d \rightarrow pp$ kinematics. Since this is not observed, the two-nucleon absorption model is consistent with the data, only if absorption takes place deep inside the nucleus allowing both nucleons to scatter on their

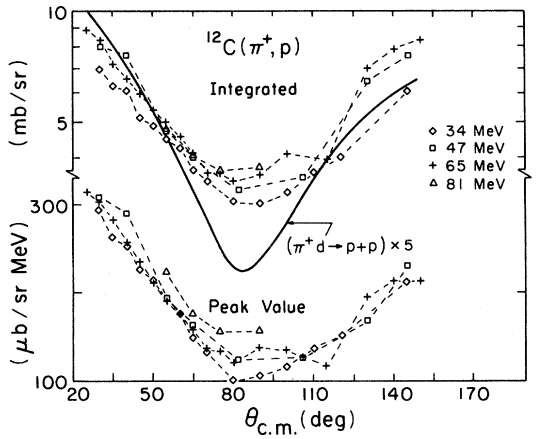

FIG. 6. The energy integrated differential cross section for $^{12}C(\pi^+,p)$ and the peak value of the double differential cross section, $d^2\sigma/dE\,d\Omega$, at 34 MeV (diamonds), 47 MeV (squares), 65 MeV (crosses), and 81 MeV (triangles). The lower limit of the energy integration is explained in the text. The differential cross section of the $\pi^+d\rightarrow pp$ at $T_\pi=47$ MeV is shown for comparison.

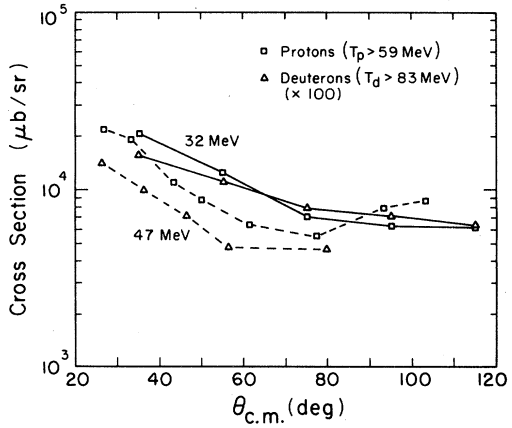

FIG. 7. Energy integrated cross sections for proton production (squares) and deuteron production (triangles) for 32 MeV pions on ^{13}C (solid lines) and 47 MeV pions on ^{12}C (dashed lines). The deuteron cross section is scaled up by 100. The low limit of integration is 59 MeV for protons and 83 MeV for deuterons.

way out. With this interpretation, the data suggests that rescattering has a larger effect on the backward angle spectra.

The maximum value of the double differential cross section $d^2\sigma/d\Omega\,dE$ at the peak of the bump is plotted in Fig. 6 as a function of scattering angle. The curve drawn is proportional to the laboratory angular distribution of the $\pi^+d\rightarrow pp$ reaction. We see that the "peak value cross section" has a shallow minimum at a scattering angle of about 90 deg, somewhat shallower than the minimum seen in the $\pi^+d\rightarrow pp$ process at the same energy. The scattering of the pion before it is absorbed, the Fermi motion of the nucleon pair on which it is being absorbed and the final state interactions of the exiting protons all tend to fill the minimum observed in the $\pi^+d\rightarrow pp$ reaction. The energy-integrated cross section shown on the same figure has a similar angular distribution. The low limit of integration was 20 to 25 MeV below the energy of the proton from the $\pi^+d\rightarrow pp$ reaction at the angle of interest. The integrated differential cross section, $d\sigma/d\Omega$, rises more at backward angles than does the double differential cross section, $d^2\sigma/d\Omega\,dE$, at the bump. In fact, the backward-to-forward angle ratio of the cross section is nearly a factor of 2 larger for the integrated cross section than for the peak cross section. This gives further evidence that the bump is more spread out at back angles, and that the effects of the nuclear medium are more important in the back angle spectra.

Another observation is that the energy dependence of the (π^+,p) cross section shown in Fig. 7 is slight, increasing by about 15% from $T_\pi=34$ to 81 MeV. The elementary $\pi^+ + d\rightarrow p + p$ cross section increases by about 60% over the same energy region.

In summary, all aspects of the inclusive $^{12}C(\pi^+,p)$ data indicate a more complicated process than a quasifree $\pi^+d\rightarrow pp$ reaction. This includes spectral shape, angular distribution, and energy dependence. Nevertheless, there is some similarity to the $\pi^+d\rightarrow pp$ process and this suggests that the two-nucleon absorption process is present, but is either not the dominant process or else is being masked by the effects of the nuclear medium.

We also have simultaneously measured continuum deuteron spectra for $E_d > 70$ MeV. There is no structure observed, and the cross section falls off monotonically for higher deuteron energies. The energy-integrated cross section for $E_d > 83$ MeV is shown in Fig. 7 along with the energy-integrated angular distributions for protons with $E_p > 50$ MeV. The deuteron cross section is forward-peaked and has approximately the shape of the proton cross section, suggestive of a pickup mechanism for deuteron production.

IV. (π^+,p) TRANSITIONS TO DISCRETE STATES

The (π^+,p) reaction brings to focus many of the leading problems in medium energy physics, in-

cluding pion absorption, off-shell behavior, and relativity. The (π^+,p) reaction to discrete states is a small part of the total pion annihilation cross section, but accounts for most of the annihilation cross section to two-body final states. The majority of (p,π) or (π,p) data have been obtained for light nuclei, specifically in the 1p shell. The purpose of this work is to add to the existing data to learn about features in the reaction mechanism. We have measured (π^+,p) cross sections on ^{12}C, ^{13}C, and ^{16}O in the energy range $32 < T_\pi < 65$ MeV. The ^{12,13}C(π^+,p)^{11,12}C data can be compared to similar data taken at $T_\pi = 90$ to 180 MeV in order to learn more about the energy dependence in the reaction. The ^{16}O(π^+,p)^{15}O data are compared to similar nuclear structure transitions in the neighboring nuclei.

The energy dependence of the ^{13}C(π^+,p)^{12}C reaction cross section to the 1^+ states at 15.1 MeV ($T=1$) and 12.7 MeV ($T=0$) is interesting. Both levels have nearly equal spectroscopic strength and are expected to be nearly identical except for their isospin difference. Anderson *et al.*[14] found that at $T_\pi = 90$ MeV the two levels are equally populated, while at $T_\pi = 170$ MeV the 15.1 MeV level is $55 \pm 14\%$ stronger. They suggested that this is an indication of a $T=\frac{3}{2}$ transfer during pion annihilation since the 15.1 MeV level may be populated by $T=\frac{1}{2}$ or $T=\frac{3}{2}$ transfer, while the 12.7 MeV level may be populated only by $T=\frac{1}{2}$ transfer. It is interesting to ask whether this isospin dependence results from the basic pion annihilation process or is a result of a multistep process. The 15.1 MeV transition may have an important two-step mechanism involving both inelastic excitation and neutron pickup. Such a two-step mechanism would favor the 15.1 MeV state over the 12.7 MeV state because the nucleon magnetic moments strongly favor $T=1$ $M1$ transitions over $T=0$ $M1$ transitions.

Interestingly, Anderson *et al.*[14,15] also show a ^{13}C(p,d)^{12}C spectrum at $T_p = 800$ MeV, $\theta = 12°$ in which the 15.1 MeV transition is about twice as strong as the 12.7 MeV transition. Since the (p,d) reaction has only $T=\frac{1}{2}$ transfer, there cannot be any difference in the 15.1 MeV ($T=1$) and 12.7 MeV ($T=0$) transitions because of isospin selection rules. We, therefore, attribute the difference in the 1^+ transition rates in the (p,d) reaction to the simple two-step process involving an isovector $M1$ inelastic excitation. We then investigated our data for evidence of a similar two-step process in the (π^+,p) reaction.

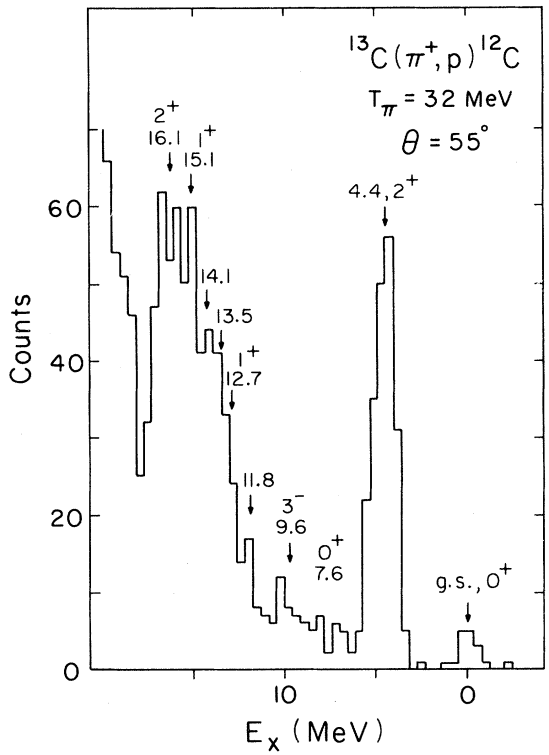

FIG. 8. The ^{13}C(π^+,p)^{12}C spectrum at $T_\pi = 32$ MeV, $\theta = 55°$.

Figures 8 and 9 show the spectra of the ^{13}C(π^+,p)^{12}C reaction at $\theta = 55°$ and 95° and $T_\pi = 32$ MeV. The resolution is about 2 MeV and is dominated by target thickness effects. With this

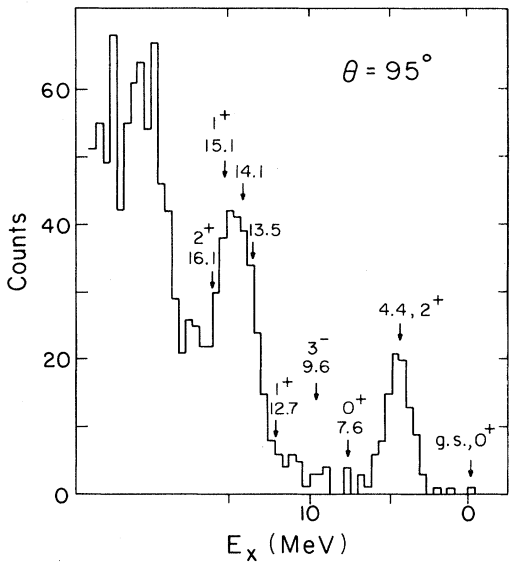

FIG. 9. The ^{13}C(π^+,p)^{12}C spectrum at $T_\pi = 32$ MeV, $\theta = 95°$.

resolution it is impossible to obtain cross sections for the 15.1 and 12.7 MeV states. However, certain qualitative observations can be made. the 15.1 MeV 1^+ state appears to be significantly stronger than the 12.7 MeV state, particularly at back angles (cf. Fig. 9).

Interestingly, Fig. 9 also demonstrates that the 4.4 MeV 2^+ state is stronger than the 16.1 MeV 2^+ ($T=1$) state, although their spectroscopic strengths are nearly equal. The relative intensities of both the 2^+ and 1^+ states suggests the importance of two-step processes involving inelastic scattering of either the initial pion or the final proton. Such inelastic processes would favor the collective 4.4 MeV 2^+ state over the 16.1 MeV 2^+ state and also favor the 15.1 MeV 1^+ state over the 12.7 MeV 1^+ state. These two-step processes become more important[16] at large momentum transfer because the inelastic process absorbs some of the momentum transfer. Therefore, it is natural that the relative differences in both the 2^+ states and 1^+ states becomes more noticeable in our backward angle spectra where the momentum transfer is largest.

The enhancement of the 4.4 MeV 2^+ state at large angles is shown in Fig. 10. The angular distribution of the 4.4 MeV state is flatter than the 0^+ ground state transition. To examine the 15.1 MeV angular distribution relative to the 16.1 MeV angular distribution we observe that the peak in the yield near 15 MeV excitation (cf. Figs. 8 and 9) shifts away from the 16.1 MeV state as the scattering angle increases. The 4.4 and 15.1 MeV angular distributions change less rapidly than the ground state and 16.1 MeV state. This is a further suggestion that two-step processes are contributing to their cross sections. Therefore, the evidence indicates that the difference between the 15.1 and 12.7 MeV states is not a $T=\frac{3}{2}$ transfer selection rule but rather the preference of an isovector $M1$ excitation over an isoscalar $M1$ excitation.

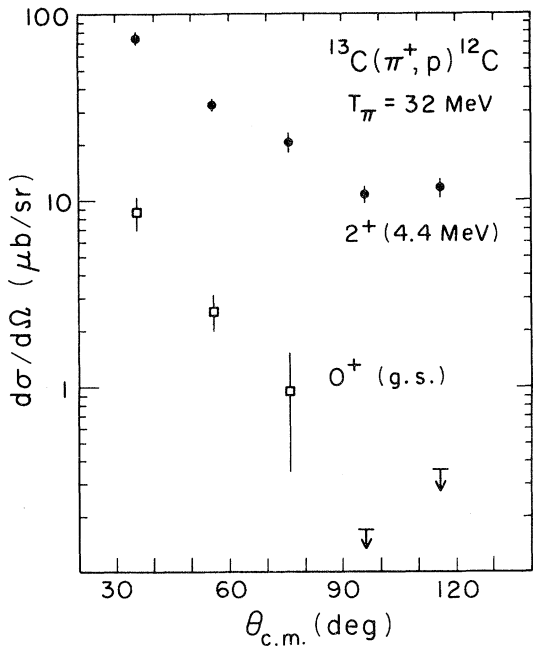

FIG. 10. The $^{13}C(\pi^+,p)^{12}C$ angular distributions to the 0^+ ground state (squares) and the 2^+ 4.4 MeV state (dots).

The dependence of the angular distributions on pion energy is interesting. Over a wide range of energies, the $^{13}C(\pi^+,p)^{12}C$(g.s.) angular distribution plotted versus momentum transfer is nearly independent of pion energy.[2] In contrast, both the $^{13}C(\pi^+,p)^{12}C$ 4.4 and 15.1 MeV angular distributions become steeper with increasing pion energy.[14] At $T_\pi=170$ MeV they both are nearly identical in shape to the ground state transition. Furthermore, the 4.4 MeV 2^+ state decreases in strength relative to the 16.1 MeV 2^+ state as the pion energy increases. We find the 4.4 MeV state to be significantly stronger than the 16.1 MeV state at $T_\pi=32$ MeV, whereas at $T_\pi=170$ MeV the 16.1 MeV state is stronger.[14] It would be interesting to try to understand this reversal in the strengths of the 2^+ states as an interference between one- and two-step processes.

We also measured the $^{12}C(\pi^+,p)^{11}C$ reaction at $T_\pi=48$ MeV (see Ref. 17) and at $T_\pi=65$ MeV. The laborabory cross section of the $^{12}C(\pi^+,p)^{11}C$ (g.s.) transition at $T_\pi=65$ MeV is 48 ± 6 μb/sr at 30° and 4.8 ± 0.5 μb/sr at 120°. In our earlier published $^{12}C(\pi^+,p)^{11}C$ work, we reported seeing a strong peak centered at 12.5 ± 0.3 MeV excitation. This peak, which was not seen in any (p,d) measurements, is interpreted as the 12.5 MeV $\frac{1}{2}^-$, $T=\frac{3}{2}$ transition which is isospin forbidden in the (p,d) reaction. This state, as pointed out earlier,[17] has a large one particle-two hole component $1p\,\frac{1}{2}$ $(1p\frac{3}{2})^{-2}$ based upon the ^{12}C core and is strongly populated in the $^{13}C(p,t)^{11}C$ reaction. The population of $T=1+|N-Z|/2$ states in the (π^+,p) reaction requires at least two nucleons in the reaction process and should provide valuable information on the reaction mechanism.

Surprisingly, this 12.5 MeV transition is not seen in any of our backward angle data or our data taken at $T_\pi=65$ MeV. It is also not seen to our knowledge, in any other $^{12}C(\pi^+,p)$ experiment,[14]

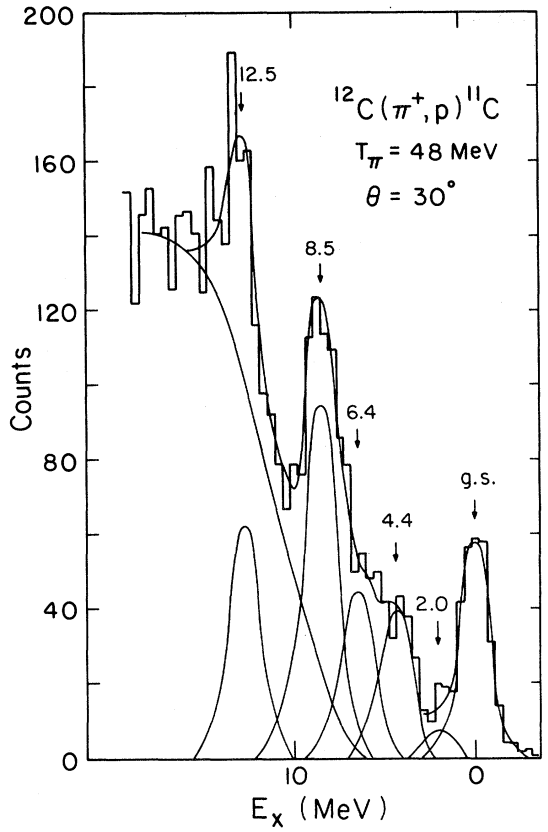

FIG. 11. A fit to the $^{12}C(\pi^+,p)^{11}C$ spectrum at $T_\pi=48$ MeV, $\theta=30°$. This spectrum was taken with our thick, 0.70 gm/cm^2, ^{12}C target.

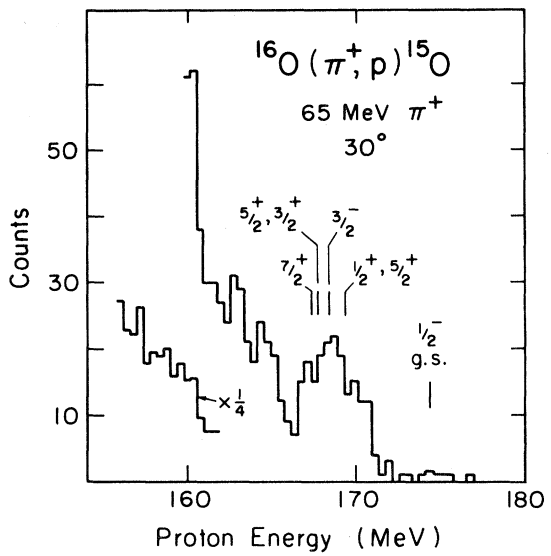

FIG. 12. The $^{16}O(\pi^+,p)^{15}O$ spectrum at $T_\pi=65$ MeV, $\theta=30°$.

thereby making it controversial. This transition has appeared in all four of our forward angle spectra at 48 MeV. Furthermore, as we changed the ^{12}C target thickness from 0.70 to 0.35 gm/cm^2 and repeated the run at $T_\pi=48$ MeV, 30°, the width of the peak narrowed with the improved energy resolution and kept the same relative intensity with respect to the other peaks in the spectrum. Our 0.70 gm/cm^2 spectrum is shown in Fig. 11. We know of no instrumental effects which could artificially create this 12.5 MeV peak, but to test the validity of this peak the experiment should be redone at the same energy and angles.

In Fig. 12 the $^{16}O(\pi^+,p)^{15}O$ spectrum at $T_\pi=65$ MeV, 30° is shown. It is surprising that the ground state transition has a laboratory cross section of only 2.3 ± 0.9 μb/sr. This transition is much weaker than other transitions in the $1p$ shell with comparable spectroscopic strength. This fact is examined by Wharton and Keister[2] who combine the data in this paper with most other available (π^+,p) or (p,π^+) data in the $1p$ shell. They show that a single neutron pickup distorted-wave calculation has serious problems in describing the systematic energy and A dependence of the cross sections of ground state transitions in the $1p$ shell. They examine the data in terms of a two-nucleon absorption model and find that features of the two-nucleon model show good possibility of describing the systematics of the data. The abnormally small $^{16}O(\pi^+,p)$ ^{15}O(g.s.) cross section can be explained by a minimum in the two-nucleon form factor.

V. (π^+,d) TRANSITIONS TO DISCRETE STATES

No (π^+,d) data to discrete states has been published. The only (π^+,d) calculations[18–20] which have been performed are based on a single-step interaction. This interaction consists of a single nucleon absorbing the pion and picking up a second nucleon immediately thereafter. The nucleon-nucleon interaction necessary to accomplish this pickup process is contained in the deuteron wave function. A one body operator of the form $\vec{\sigma}\cdot\vec{\nabla}_\pi$ is used for the absorption of the pion on the nucleon. With this operator, a proper antisymmetrization of the target wave function leads to the following selection rule: The two initial neutrons have relative (internal) angular momentum l=even for a singlet state ($S=0$) and l=odd for a triplet state ($S=1$). The reaction mechanism prefers the two target neutrons to be close to each other in a

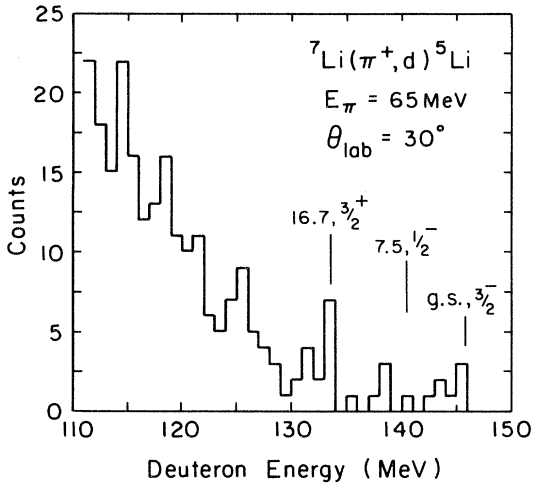

FIG. 13. The ^{7}Li(π^+,d)^{5}Li spectrum at T_π=65 MeV, θ=30°. Each count above 120 MeV represents about 54 nb/sr.

l=0 state, thereby favoring the annihilation on a singlet dineutron. Betz and Kerman[19] calculate that the S=1 transitions are a factor of 100 weaker than the S=0 transitions.

Another prediction of the Betz-Kerman calculation is that the ^{18}O(π^+,d)^{16}O(g.s.)0$^+$ transition should be a factor of 10 larger than either the ^{12}C(π^+,d)^{10}C(g.s.)0$^+$ or the ^{10}C(3.36 MeV)2$^+$ transition. The prediction comes from two effects: (1) the ^{18}O ground state is a well known pairing condensate with constructive, coherent mixture of $(1d_{5/2})^2$, $(1d_{3/2})^2$, and $(2s_{1/2})^2$ configurations, (2) the $(2s_{1/2})^2$ and $(1d_{3/2})^2$ (π^+,d) transition matrix elements are very large. For these two nuclear structure effects to be applicable they must be extrapolated to a region of nuclear structure in which a pair of neutrons are moving together in the target at small relative momentum but large total momentum (~800 MeV/c) with respect to the rest of the nucleus. This is a totally unexplored region of nuclear structure.

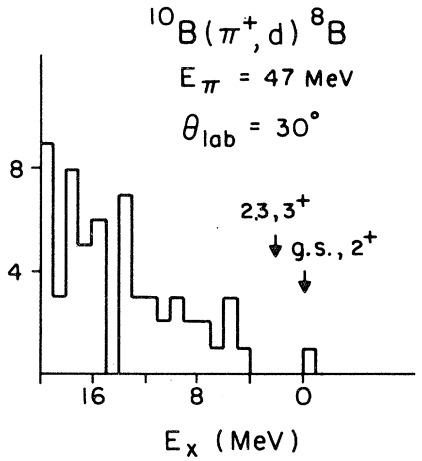

FIG. 14. The ^{10}B(π^+,d)^{8}B spectrum at T_π=47 MeV, θ=30°. Each count represents about 72 nb/sr.

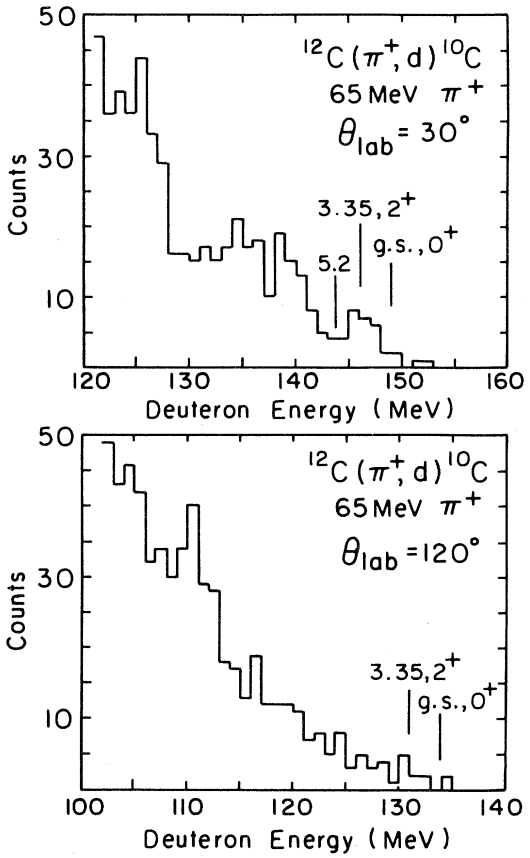

FIG. 15. The ^{12}C(π^+,d)^{10}C spectra at T_π=65 MeV, θ=30° and 120°. Each count above 120 MeV represents about 15 nb/sr at θ=30° and 16 nb/sr at θ=120°.

There are many other predictions by Betz and Kerman, but the two examples above are representative of the information we wish to obtain about the (π^+,d) reaction. The prediction on spin transfer is intimately related to the reaction mechanism, whereas the prediction on ^{18}O(π^+,d)^{16}O(g.s.) is both a question of reaction mechanism and nuclear structure. In addition to exploring the many predictions of the Betz-Kerman theory, we also wish to make an empirical comparison of the (π^+,d) data with the (π^+,p) data to observe similarities and differences between the two reactions.

Our experimental apparatus allowed us to collect the (π^+,d) data simultaneously with the (π^+,p)

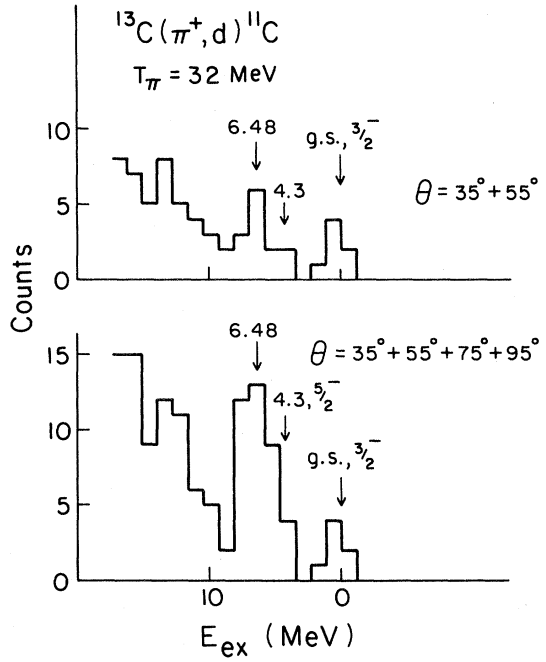

FIG. 16. The $^{13}C(\pi^+,d)^{11}C$ spectra at $T_\pi=32$ MeV. At the top is the sum of $\theta=35°$ and 55° spectra. At the bottom is the sum of 35°, 55°, 75°, and 95° spectra. Only a few of the ^{11}C states are labeled (see Fig. 11).

data. The particle identification (see Fig. 4) was good enough to obtain essentially pure deuteron spectra. These spectra are shown in the order of the target masses in Figs. 13–18. The (π^+,d) reaction is similar to the (p,t) reaction since both involve two-neutron pickup. In contrast to the (p,t) reaction where $0^+\rightarrow0^+$ ground state transitions often dominate the spectra, no such transitions are clearly identifiable in the (π^+,d) spectra. There are no counts in the region of the 0^+ ground state for all $^{18}O(\pi^+,d)^{16}O$ (Fig. 18) and $^{16}O(\pi^+,d)^{14}O$ (Fig. 17) spectra. There is some hint of the $^{12}C(\pi^+,d)^{10}C$ 0^+ ground state transition in Fig. 15, but it is weak and not clearly resolved from the transition to the $^{10}C(3.36)2^+$ state. Because of the poor statistics, energy resolution (2.0–3.0 MeV), and the 0.5 MeV uncertainty in the absolute energy calibration (see Sec. II B), it is difficult to resolve and identify nearby states.

These $0^+\rightarrow0^+$ transitions are necessarily zero angular momentum transfer, ($L=0$) processes. If the dominant pion partial waves are $l_\pi=0$, 1, 2,

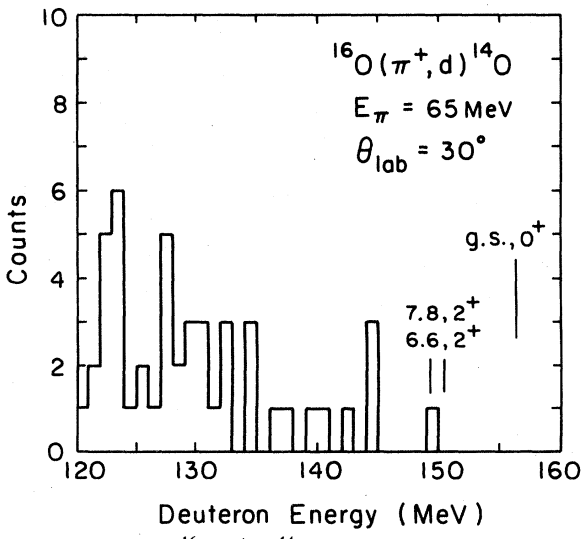

FIG. 17. The $^{16}O(\pi^+,d)^{14}O$ spectrum at $T_\pi=65$ MeV, $\theta=30°$. Each count represents about 246 nb/sr. The labeled states are the strongest transitions seen in the $^{16}O(p,t)^{14}O$ reaction.

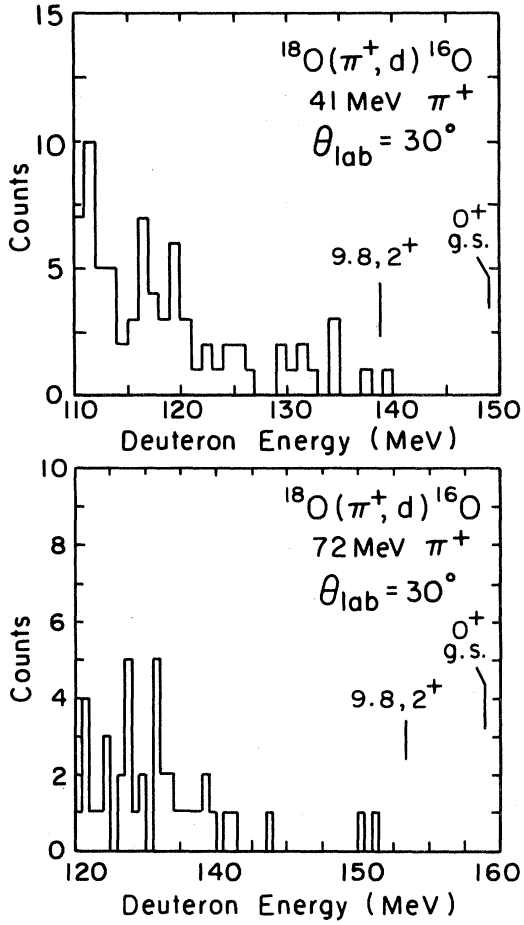

FIG. 18. The $^{18}O(\pi^+,d)^{16}O$ spectra at $T_\pi=41$ and 72 MeV, $\theta=30°$. Each count in the 41 MeV spectrum above 120 MeV is about 156 nb/sr. Each count in the 72 MeV spectrum is about 260 nb/sr. There are other states in the vicinity of the 9.8 MeV 2^+.

TABLE I. $L=2(\pi^+,d)$ cross sections.

Final state	T_π	θ_d	$q(\pi,d)$ (MeV/c)	$\frac{d\sigma}{d\Omega}(\pi^+,d)$ (μb/sr)	$\frac{d\sigma}{d\Omega_{max}}(p,t)$ (mb/sr)	$\frac{d\sigma(\pi^+,d)}{d\sigma(p,t)}$ ($\times 10^{-3}$)	Reference (p,t) data
^{8}B(g.s.)2^+	48	30	607	$\lesssim 0.07$	0.09		22
^{10}C(3.36)2^+	48	30	603	0.51 ± 0.21	0.22		23
	65	30	625	0.30 ± 0.07		1.4	
^{11}C(g.s.)$\frac{3}{2}^-$	32	35	626	$1.6\ \pm0.8$	1.0	1.6	24
^{14}O(6.59)2^+ (7.78)2^+	65	30	639	$\lesssim 0.24$	0.2		25
^{16}O(9.85)2^+	41	30	651	$\lesssim 0.16$	0.12		26
	72	30	686	$\lesssim 0.26$			

then angular momentum conservation restricts the deuteron impact parameter to less than 0.5 fm. In contrast, a $L=2$ transition would allow deuteron impact parameters larger than 1.0 fm. The only $L=0$ transition which is clearly identifiable in our spectra is the ^{7}Li$(\pi^+,d)^5$Li(g.s.) $\frac{3}{2}^- \rightarrow \frac{3}{2}^-$ transitions (Fig. 13). At $T_\pi=65$ MeV $\theta=30°$ the laboratory cross section for this transition is about 0.22 ± 0.06 μb/sr. Although this transition is predominantly $L=0$ it also has a 1 $L=2$ amplitude, as shown in the (p,t) data of Cerny *et al.*[21]

Removing two neutrons from the p shell restricts the angular momentum transfer to 0 and 2. Our spectra clearly show that the $L=2$ transitions are generally much stronger than the $L=0$ transitions. Data at forward angles on five of these transitions: ^{10}B$(\pi^+,d)^8$B(g.s.)2^+, ^{12}C$(\pi^+,d)^{10}$C(3.36)2^+, ^{13}C$(\pi^+,d)^{11}$C(g.s.)$\frac{3}{2}^-$, ^{16}O$(\pi^+,d)^{14}$O(6.6 and 7.8)2^+, and ^{18}O$(\pi^+,d)^{16}$O(9.85)2^+ are given in Table I. The (p,t) reaction at $T_p\sim45$ MeV shows a nearly pure $L=2$ angular distribution for all five of these transitions, with a maximum in the angular distribution occurring near 25°. The (p,t) cross section at this maximum is given in column 5 of Table I. The two transitions with the best (π^+,d) statistics, ^{10}C(3.36)2^+ and ^{11}C(g.s.)$\frac{3}{2}^-$ give the same relative strength as do the (p,t) reactions at $T_p=40$ MeV. For both types of reactions the ^{11}C (g.s.) transition is a factor of 5 larger than the ^{10}C(3.36) transition even though the momentum transfer is quite different, 625 MeV/c for the (π^+,d) and 140 MeV/c for the (p,t) reactions. Since it is known that the (p,t) cross sections agree well with the shell model calculations of the spectroscopic strength, we can tentatively conclude that the (π^+,d) cross sections are also proportional to the spectroscopic strength. It should be emphasized that a proper comparison of the strengths of various (π^+,d) transitions should be made at the same momentum transfer. Smaller momentum transfer is expected to result in larger cross sections.

The Betz and Kerman calculation,[19] which includes distortion in both the pion and deuteron wave functions, seriously misses the L dependence of the (π^+,d) cross section. The ^{12}C$(\pi^+,d)^{10}$C(3.36 MeV)2^+ transition is at least a factor of 4 larger than the ^{12}C$(\pi^+,d)^{10}$C(g.s.)0^+ transition. In contrast, the calculation shows the 2^+ transition to be only 20–40% larger than the 0^+ transition. The calculation also predicts the ^{18}O$(\pi^+,d)^{16}$O(g.s.)0^+ transition to be a factor of 10 larger than either the ^{12}C$(\pi^+,d)^{10}$C(g.s.) or the ^{10}C(3.36 MeV) transition. In contrast, observation shows it to be at least a factor of 2 weaker than the ^{10}C(3.36 MeV) transition. Part of this latter disagreement may be attributable to the nuclear structure questions referred to earlier, but there is certainly a disagreement with the predicted L dependence of the cross section. The dominant contribution to the L dependence is possibly the attenuation of the deuteron distorted wave. This attenuation favors a surface reaction resulting in a large angular momentum mismatch of the deuteron with the pion. If the attenuation is large, the L transfers which allow a smaller mismatch closer to the surface will be favored, thereby favoring $L=2$ over $L=0$. The L dependence of the cross section depends on the imaginary part of the deuteron optical potential which is not well known near $T_d=200$ MeV. Betz and Kerman find that the uncertainties in the ima-

ginary part of the deuteron potential can lead to a factor of 10 change in the $L=0$ cross sections at forward angles. Basically, this large effect occurs because Betz and Kerman find the main contribution to the (π^+,d) reaction comes from the inner region of the nucleus where the attenuation is greatest. The strong L dependence, which we observe in the (π^+,d) reaction, may ultimately provide information on the imaginary part of the deuteron optical potential deep inside the nucleus.

Having examined the enhancement of $L=2$ transfer to $L=0$ for the (π^+,d) reaction, we turn to the spin dependence of the reaction. The (p,t) reaction can pick up two neutrons only in an $S=0$ state. $S=1$ transitions are, in addition, allowed for the (π^+,d) reaction. To examine the spin dependence, we look at the ^{7}Li$(\pi^+,d)^5$Li reaction. The only narrow state which is known to exist in the particle unstable ^{5}Li nucleus is the $\frac{3}{2}^+$ state at 16.7 MeV. This state is known[27] to be a two-particle-one hole state with the configuration $^{2S+1}I_J = {}^4S_{3/2}$. Since the ^{7}Li ground state is $^2P_{3/2}$, the transition between the two states must be $S=1$, $L=1$. In the (p,t) reaction it is forbidden and not seen.[21] However, in the ^{7}Li$(p,^3$He$)^5$He reaction, for which $S=1$ is allowed, the analog transition to the 16.7 MeV $\frac{3}{2}^+$ is dominant in the ^{5}He spectrum.[21] Interestingly there is a statistically questionable peak in the ^{7}Li$(\pi^+,d)^5$Li spectrum in Fig. 13, centered at $E_x=17$ MeV. The only other states besides the 16.7 MeV $\frac{3}{2}^+$ state known to exist in this vicinity are very broad states at $E_x=18$ and 20 MeV. The seven counts in the peak correspond to 0.4 μb/sr at $T_\pi=65$ MeV, $\theta_{\text{lab}}=30°$. Such a strong population of a $S=1$ transition would be incompatible with the model of Betz and Kerman.

Next, we examine the ^{13}C$(\pi^+,d)^{11}$C spectra in Fig. 16. In addition to the ^{11}C(g.s.) peak there is a peak in the vicintiy of the 6.48 MeV $\frac{7}{2}^-$ and 4.3 MeV $\frac{5}{2}^-$ states, which are more evident in the spectra at back angles. These states are well described as ^{12}C(4.4)$2^+ \otimes 1p_{3/2}{}^{-1}$ configurations and are strongly seen in the other large momentum transfer pickup reactions (π^+,p) and (p,d).[17] These states have small spectroscopic strength for both single neutron and two neutron pickup reactions and presumably are populated through two-step processes involving inelastic quadrupole excitation. Such two-step processes become more significant at large momentum transfer because the inelastic process can absorb some of the momentum transfer. The (π^+,d) angular distribution to these $\frac{7}{2}^-$ and

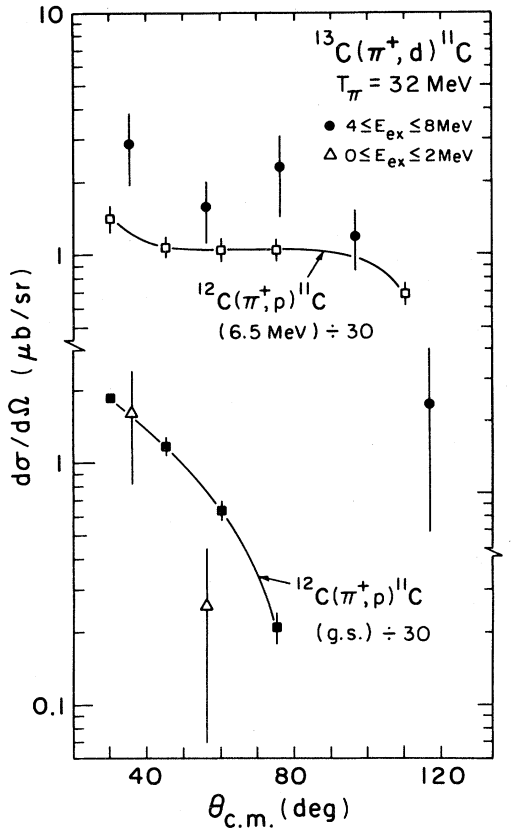

FIG. 19. Angular distributions for the ^{13}C$(\pi^+,d)^{11}$C reaction at $T=32$ MeV. The angular distributions of the ^{12}C$(\pi^+,p)^{11}$C reaction at $T_\pi=48$ MeV to the same states is shown for comparison.

$\frac{5}{2}^-$ states are less forward peaked than the ground state transition (Fig. 19). There is a very strong similarity between the (π^+,d) and (π^+,p) cross sections to these states. Firstly, the shapes of their angular distributions are nearly identical for both reactions and secondly, the strength of these $\frac{7}{2}^-$ and $\frac{5}{2}^-$ states relative to the $\frac{3}{2}^-$ g.s. transition is nearly the same for both the (π^+,d) and (π^+,p) reaction. The ^{12}C$(\pi^+,p)^{11}$C angular distributions are included in Fig. 19 for comparison. It is remarkable that the relative importance of two-step processes with respect to one-step processes appears nearly identical for the (π^+,d) and (π^+,p) reactions.

Lastly, we wish to compare the experimental angular distributions with the calculations by Betz and Kerman[19] for the pure $L=2$ two-neutron removal transitions. Betz and Kerman find that

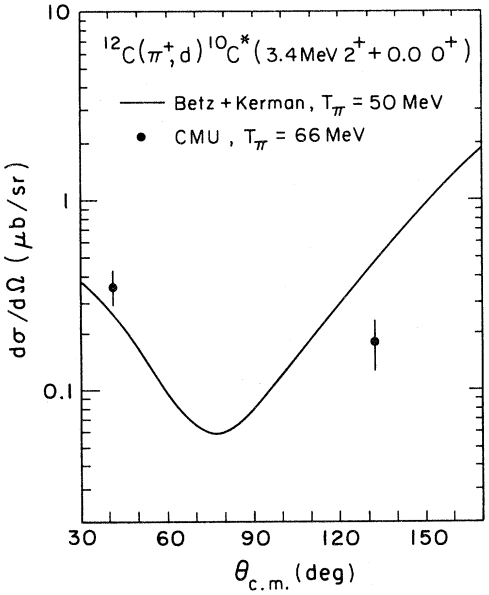

FIG. 20. The angular distribution of the $^{12}C(\pi^+,d)^{10}C$ reaction to the 0^+ g.s. and 3.35 MeV 2^+ state. The data is at $T_\pi=66$ MeV and the calculation (Ref. 19) is at $T_\pi=50$ MeV.

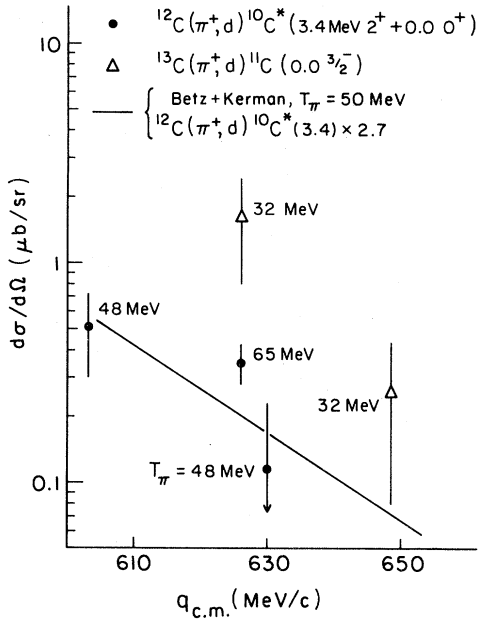

FIG. 21. The dependence of the forward angle differential (π^+,d) cross section on momentum transfer. The data were taken at several pion energies (as labeled) and the calculation (Ref. 19) is at $T_\pi=50$ MeV.

both pion and deuteron distortion have a strong effect on the shape and magnitude of the angular distributions. the off-shell propagation of the pion increases the calculated cross section at large momentum transfer (large angles) relative to the Born approximation. The strong damping of the deuteron wave in the nuclear medium suppresses the forward angle cross section by almost three orders of magnitude. The net effect is that the (π^+,d) differential cross section is largest at 180°. We checked this by measuring the $^{12}C(\pi^+,d)^{10}C$ cross section at 30° and 120°. The differential cross section to the 0^+ g.s. plus 2^+ 3.35 MeV states at $T_\pi=65$ MeV are shown in Fig. 20 along with the Betz and Kerman calculations at 50 MeV. The magnitude and shape of the angular distribution are well reproduced.

Next we investigate the shape of the angular distribution at forward angles. The (π^+,p) cross sections to states with large spectroscopic strength in the $1p$ shell obey a simple exponential behavior[2] with momentum transfer, q, at forward angles: $\sigma(\theta)=Ce^{-\lambda q}$. Interestingly, Betz and Kerman predict a similar exponential behavior for the (π^+,d) reaction but with a slope, $\lambda=(22$ MeV/$c)^{-1}$, which is twice as steep as observed[2] in $^{12}C(\pi^+,p)$, (41 MeV/$c)^{-1}$. Experimentally, the data give even a steeper slope but with the large error bars are consistent with the calculation (Fig. 21).

Betz and Kerman also make a prediction that the (π^+,d) forward angle cross section increases a factor of 10 from $T_\pi=50$ to 87.5 MeV. However, the data for $^{12}C(\pi^+,d)^{10}C(3.36)$, $\theta=30°$, show no increase in cross section between $T_\pi=49$ and 65 MeV.

The model for the (π^+,d) reaction has shown both success and failure in describing the data. Whether the successes, such as predicting the approximate magnitude of the cross section, are fortuitous or indicative of the model's basic validity must await further study.

VI. SUMMARY

In this paper we have presented (π^+,p) and (π^+,d) data on $1p$ shell nuclei populating both discrete states and the continuum. By examining the features of the data we make the following observations: (1) The (π^+,p) data to discrete states show the importance of two-step processes involving inelastic scattering. (2) The ^{16}O (π^+,p) ^{15}O(g.s.) transition is abnormally small. The (π^+,p) data to the continuum show characteristics which are only weakly suggestive of a two-nucleon

absorption process. A determination of the basic reaction process will require a careful study of nuclear structure effects such as Fermi momentum and final state interactions of the two outgoing protons (12). The (π^+,d) continuum data are also presented and show nearly identical angular dependence as the (π^+,p) continuum data. (4) The first (π^+,d) data to discrete states is also published. Transitions to several states with measurable spectroscopic strength for the removal of two neutrons coupled to angular momentum $L=2$ are seen. The angular distributions are forward peaked showing a steep exponential fall-off with momentum transfer. No $L=0$ transitions are unambiguously identified. (5) Additional transitions which are known to be predominantly two-neutron removal coupled to a strong collective quadrupole excitation are seen. These multistep transitions have cross sections which are nearly isotropic between 35 and 100 deg in sharp contrast to the strong forward peaking of the pure $L=2$ two-neutron removal transitions. There is a striking similarity with the (π^+,p) angular distributions to the same final states.

The (π^+,d) data are compared to the DWBA calculations of Betz and Kerman. The DWBA calculations successfully predict the magnitude and shape at forward angles for the angular distributions of the $L=2$ transitions. However, the DWBA calculation seriously underestimates the L dependence of the (π^+,d) cross section and overestimates the cross section dependence on pion energy. The theory should be reexamined and attempts made to reconcile it with the data. It may be possible to reconcile the theory with experiment without significantly altering the assumed reaction mechanism. However, a fundamental prediction of the theory[18,19] is that $S=1$ transitions are strongly suppressed. There is an indication of the $S=1$ ^{7}Li(π^+,d)^{5}Li(16.7 MeV) $\frac{3}{2}^+$ transition in the data. (If the peak at 16.7 MeV excitation in the ^{5}Li spectrum is not a statistical fluctuation, then the theoretical model of the basic reaction mechanism will need to be revised.) The ^{7}Li(π^+,d)^{5}Li reaction is being studied in a current experiment at LAMPF (Ref. 28) to clarify the issue.

ACKNOWLEDGMENTS

We would like to acknowledge the participation in the development of the germanium detector of J. Anderson, D. Cordi, F. Goulding, E. Haller, D. Landis, J. Lin, N. Madden, and D. Malone. We would also like to acknowledge the financial support of the U. S. Department of Energy (USDOE) and to thank the staff of LAMPF for help in mounting the experiment. Finally, we would like to thank L. S. Kisslinger, B. D. Keister, M. Betz, and A. Kerman for helpful discussions about the theory.

---

*Present address: Nuclear Physics Laboratory, University of Washington, Seattle, Washington 98195.

†Present address: Physics Department, Massachusetts Institute of Technology, Cambridge, Massachusetts 02139.

‡Present address: Tandem Lab, Niels Bohr Institute, Riso 4000 Roskilde, Denmark.

§Present address: Department of Physics, Kyoto-Sangyo University, Kamigamo Motoyama, Kyoto 603 Japan.

[1]B Höistad, Adv. Nucl. Phys. 11, 135 (1979); D. F. Measday and G. A. Miller, Annu. Rev. Nucl. Part. Sci. 29, 121 (1979); H. W. Fearing (unpublished).

[2]W. R. Wharton and B. D. Keister, Phys. Rev. C 23, 1141 (1981).

[3]H. E. Jackson, S. B. Kaufman, L. Meyer-Schützmeister, J. P. Schiffer, S. L. Tabor, S. E. Vigdor, J. N. Worthington, L. L. Rutledge, Jr., R. E. Segel, R. L. Burman, P. A. M. Gram, R. P. Redwine, and M. A. Yates, Phys. Rev. C 16, (1977).

[4]R. D. McKeown, S. J. Sanders, J. P. Schiffer, H. E. Jackson, M. Paul, J. R. Specht, E. J. Stephenson, R. P. Redwine, and R. E. Segel, Phys. Rev. Lett. 44, 1033 (1980); R. D. McKeown, J. P. Schiffer, H. E. Jackson, M. Paul, S. J. Sanders, J. R. Specht, E. J. Stephenson, R. P. Redwine, R. E. Segel, J. Arends, J. Eyink, H. Hartmann, A. Hegerath, B. Mecking, G. Nöldeke, and H. Rost, *ibid.* 45, 2015 (1980).

[5]R. L. Burman, R. L. Fulton, and M. Jakobson, Nucl. Instrum. Methods 131, 29 (1975).

[6]J. F. Amann, P. D. Barnes, K. G. R. Doss, S. A. Dytman, R. A. Eisenstein, J. D. Sherman, and W. R. Wharton, Phys. Rev. C 23, 1635 (1981).

[7]K. G. R. Doss, Carnegie-Mellon University Internal Report COO-3244-42 and Ph.D. thesis, 1980 (unpublished).

[8]R. Eisberg, D. Ingham, M. Makino, R. Cole, and C. Waddell, Nucl. Instrum. Methods 146, 487 (1977).

[9]P. Y. Bertin, B. Coupat, A. Hivernat, D. B. Isabelle, J. Duclos, A. Gerard, J. Miller, J. Morgenstern, J. Pi-

card, P. Vernin, and R. Powers, Nucl. Phys. B106, 431 (1976).
[10]D. C. Dodder, private communication.
[11]B. M. Preedom, C. W. Darden, R. D. Edge, T. Marks, M. J. Saltmarsh, K. Gabathuler, E. E. Gross, C. A. Ludemann, P. Y. Bertin, M. Blecher, K. Gotow, J. Alster, R. L. Burman, J. P. Perroud, and R. P. Redwine, Phys. Rev. C 17, 1402 (1978); C. Richard-Serre, W. Hirt, D. F. Measday, E. G. Michaelis, M. J. Saltmarsh, and P. Skarek, Nucl. Phys. B20, 413 (1970).
[12]K. G. R. Doss and W. R. Wharton, Phys. Rev. C 22, 1219 (1980).
[13]Che Ming Ko and S. Bohrmann, Phys. Lett. 97B, 188 (1980).
[14]R. E. Anderson, B. Höistad, R. L. Boudrie, E. W. Hoffmann, R. J. Macek, C. L. Morris, H. A. Thiessen, G. R. Smith, and J. Källne, Phys. Rev. C 23, 2616 (1981).
[15]G. R. Smith, J. R. Shepard, R. J. Peterson, and N. J. Digiacomo, Bull. Am. Phys. Soc. 23, 951 (1978); private communication.
[16]J. Källne and A. W. Obst, Phys. Rev. C 15, 477 (1977).
[17]J. F. Amann, P. D. Barnes, K. G. R. Doss, S. A. Dytman, R. A. Eisenstein, J. D. Sherman, and W. R. Wharton, Phys. Rev. Lett. 40, 758 (1978).
[18]R. A. Eisenstein and G. A. Miller, Phys. Rev. C 11, 2001 (1975).
[19]M. Betz and A. K. Kerman, Nucl. Phys. A345, 493 (1980).
[20]M. Dillig, C. Helwig, and M. G. Huber, Nuovo Cimento 18, 487 (1977).
[21]J. Cerny, C. Detraz, and R. H. Pehl, Phys. Rev. 152, 950 (1966).
[22]G. T. Squier, A. R. Johnston, E. W. Spiers, S. A. Harbison, and N. M. Stewart, Nucl. Phys. A141, 158 (1970).
[23]W. Benenson, G. M. Crawley, J. D. Dreisbach, and W. P. Johnson, Nucl. Phys. A97, 510 (1967).
[24]S. Micheletti, M. Pignanelli, and P. Guazzoni, Phys. Rev. C 11, 64 (1975).
[25]J. A. Macdonald, J. Cerny, J. C. Hardy, H. L. Harney, A. D. Bacher, and G. R. Plattner, Phys. Rev. C 9, 1694 (1974).
[26]M. Pignanelli, S. Micheletti, I. Iori, P. Guazzoni, and F. G. Resmini, Phys. Rev. C 10, 445 (1974).
[27]K. Ramavataram and S. Ramavataram, Nucl. Phys. A147, 293 (1970).
[28]LAMPF Experiment No. 315, W. R. Wharton.